Published in final edited form as:
FEBS Lett. 2013 November 1; 587(21): . doi:10.1016/j.febslet.2013.08.035.

Understanding inositol pyrophosphate metabolism and function: kinetic characterization of the DIPPs

Rajagopal S. Kilari[1], **Jeremy D. Weaver**[2], **Stephen B. Shears**[2], and **Stephen T. Safrany**[1]

[1]Department of Pharmacy, Faculty of science and Engineering, University of Wolverhampton Wulfruna Street, Wolverhampton, WV1 1LY, U.K

[2]Inositide Signaling Group, Laboratory of Signal Transduction, National Institute of Environmental Health Sciences, NIH, Research Triangle Park, PO Box 12233, NC 27709, U.S.A

Abstract

We illuminate inositol pyrophosphate turnover and cell-signaling activities, by showing that regulation of yeast cyclin-kinase by 1-InsP_7 is not conserved for mammalian CDK5, and by kinetically characterizing Ddp1p/DIPP-mediated dephosphorylation of 1-InsP_7, 5-InsP_7 and InsP_8. Each phosphatase exhibited similar K_m values for every substrate (range: 35-148 nM). The rank order of k_{cat} values (1-InsP_7 > 5-InsP_7 = InsP_8) was identical for each enzyme, although DIPP1 was 10-60 fold more active than DIPP2α/β and DIPP3α/β. We demonstrate InsP_8 dephosphorylation preferentially progresses through 1-InsP_7. Conversely, we conclude that the more metabolically and functionally significant steady-state route of InsP_8 synthesis proceeds via 5-InsP_7.

1. Introduction

Among the many members of the inositol phosphate signaling family, the diphosphoinositol polyphosphates (inositol pyrophosphates;1-InsP_7, 5-InsP_7 and InsP_8) receive particular attention. These “high-energy” signals operate at the interface of cell signaling and metabolic homeostasis [1,2], by phosphorylating proteins [3] (but see [4]), by regulating transcriptional responses to environmental stress [5-7], and by modulating PtdIns(3,4,5)P_3-signaling [8,9].

Understanding metabolic regulation of inositol pyrophosphate turnover reveals how this signaling cascade is controlled. Indeed, no metabolic pathways can be modeled accurately without knowledge of the kinetic parameters of the participating enzymes [10]. Inositol pyrophosphate metabolism is complicated by the two kinase pathways from InsP_6 to InsP_8 (I and II; ref [11] and Fig. 1), and by diphosphoinositol polyphosphate phosphohydrolases (DIPPs). Another confounding factor is that humans express five DIPP isoforms: types 1, 2α, 2β, 3α and 3β [12-15] *S. cerevisiae* only express one: the diadenosine and diphosphoinositol phosphohydrolase (Ddp1p) [16]. Little is known concerning the Michaelis-Menten kinetic parameters for Ddp1p/DIPPs; no such data are published for 1-InsP_7 and InsP_8. While some kinetic data have been provided for 5-InsP_7, their reliability is now being questioned. For instance, K_m values for 5-InsP_7 vary from 4 nM for DIPP1 [12] to 4 μM for DIPP3β [15]. Such variation seems inconsistent with the high conservation of

Authors' email for correspondence: shears@niehs.nih.gov; S.Safrany@wlv.ac.uk.

DIPP's catalytic domain. Instead, recent improvements in enzymatic [17] and chemical [18,19] methods for synthesizing inositol pyrophosphates have called into question the quality of some early sources of 5-$InsP_7$ (see [18]). Here, using improved methods for the enzymatic synthesis and electrophoretic purification of 1-$InsP_7$, 5-$InsP_7$ and $InsP_8$ [17], we have kinetically characterized the DIPP family.

2. Methods and Materials

2.1 Materials

GST-DIPP3α and GST-DIPP3β were prepared as described [15]. GST-DIPPs 1, 2α and 2β plasmids [12,13] were subcloned from pQE30 into pGEX6P-1 using BamHI and SalI. Expression plasmids were transformed into *E. coli* (BL21), and induced at 26°C overnight with 100 μM IPTG. Cells were harvested and sonicated in 20 mM Tris, 150 mM NaCl, 2 mM DTT, 0.1 mM EGTA, pH 7.5, 5 μg/ml leupeptin and 1 μg/ml aprotinin. GST-DIPPs were then purified using a Glutathione Sepharose-4 Fast-Flow column (Amersham Pharmacia Biotech). Protein was stored at −80°C in 10% v/v glycerol. Professor A.G. McLennan kindly provided Ddp1p.

The CDK5RAP1 open-reading frame was PCR-amplified from IMAGE clone 4418659, subcloned into pENTR/TEV/D-TOPO, and further subcloned into pDest606 in *E. coli* (DH5α). The CDK5RAP1-pDest606 construct was transformed into *E. coli* DH10Bac cells, yielding CDK5RAP1/bMON14272 bacmid; this was amplified by successive infections of Sf9 cells, then used to infect Sf9 cells for protein expression. After 72 hr., cells were lysed in I-Per (Pierce) plus protease inhibitor cocktail (Roche). CDK5RAP1 was purified using Ni-NTA resin and then an amylose resin column. Protein was stored at −80°C.

$InsP_6$ was obtained from Calbiochem. Enzymatically-prepared inositol pyrophosphates were electrophoretically purified [17,20]. Samples from “blank” gels (i.e. no inositol pyrophosphates), processed in parallel, provided vehicle controls. Purity (by HPLC) of 5-$InsP_7$, 1-$InsP_7$, and $InsP_8$ was, respectively, 86%, 95% and 94%. Such slight decomposition of the pyrophosphate groups does not significantly affect assays of DIPP activity [19]. Assays were corrected for the “zero-time” products.

2.2 Assays

Phosphatase activity was determined at 30°C (Ddp1p) or 37°C (DIPPs) in 20 μl of buffer containing 50 mM KCl, 50 mM HEPES (pH 7.2 with KOH), 4 mM CHAPS, 0.05 mg/ml BSA, 1 mM Na_2EDTA, 2 mM $MgSO_4$. [^{3}H]labeled and non-radiolabeled $InsP_7$ or $InsP_8$ [20] were added as indicated (see Figures). After 2-25 min (corresponding to approx. 20% substrate metabolism), reactions were quenched and neutralized [14], loaded onto a HiChrom 4.6 × 125 mm Partisphere SAX column, and eluted (1 ml/min) with one of two protocols generated by mixing Buffer A (1 mM Na_2EDTA) with buffer B [A + 1.3 M $(NH_4)_2HPO_4$, pH 3.85 with H_3PO_4]: protocol 1), 0–5 min, B=0%; 5–10 min, B=0–45%; 10–55 min, B=45-100% (1ml fractions); protocol 2), 0–5 min, B=0%; 5–10 min, B=0–50%; 10–55 min, B=50-100% (0.5ml fractions). [^{3}H] was assayed by liquid scintillation spectrometry. K_m and k_{cat} values were obtained by non-linear regression.

CDK5 activity was measured after preincubating (30 min) 50 ng CDK5/p35 (Sigma) and 20 ng CDK5RAP1 in 45 μl reactions containing 20 mM MOPS pH 7.4, 1 mM EGTA, 20 mM $MgCl_2$, 1 mM dithiothreitol, 100 μM (γ-^{32}P)ATP (0.05 μCi) and the appropriate inositol phosphate. Reactions were initiated with 5 μl of 1 mg/ml peptide substrate (BioMol International). After 30 min, 40 μl of each reaction was quenched by spotting onto P81 phospho-cellulose filters (Millipore). These were washed (4×; 0.75% H_3PO_4) and acetone-rinsed. [^{32}P] was assayed by Cerenkov counting.

3. Results and Discussion

3.1 Ddp1p kinetics

By HPLC analysis of the dephosphorylation of [^{3}H]-radiolabeled substrates, we have kinetically characterized recombinant Ddp1p from *S. cerevisiae*. Ddp1p hydrolyzed 1-InsP_7 and 5-InsP_7 to InsP_6 (Fig 2A,B). InsP_8 was dephosphorylated to InsP_6, with relatively little accumulation of InsP_7 (Fig. 2C, and see below). Substrate saturation plots (Fig. 2) showed that K_m values for each substrate were very similar (93nM, 105 nM, 148 nM; Table 1), but 1-InsP_7 was hydrolyzed at a 5 to 6-fold faster rate than 5-InsP_7 and InsP_8 (Table 1).

No previous studies have described Michaelis-Menten kinetic parameters for Ddp1p activity towards either 1-InsP_7 or InsP_8. There is one earlier study [21] that incubated Ddp1p with 250 μM of either 1-InsP_7 or 5-InsP_7; in an electrophoretic analysis, only 1-InsP_7 was found to be dephosphorylated. That inability to detect 5-InsP_7 metabolism may have reflected its assay concentration exceeding the K_m value by 3 orders of magnitude (see Table 1). Also, SDS-PAGE mass analysis is less sensitive than is HPLC analysis of [^{3}H]-labeled substrates. So although the preference of Ddp1p for 1-InsP_7 over 5-InsP_7 was previously known [21], our new kinetic data indicate the relative reaction rates are closer than previously suggested.

3.2 Human DIPP kinetics

We obtained substrate saturation plots (not shown) to derive K_m and k_{cat} values for all five human DIPPs (Table 1). DIPP1 exhibited the highest k_{cat}, irrespective of substrate (Table 1). Thus, for example, the relative levels of cellular expression of DIPP1, versus the 20 to 60-fold less active DIPP2 isoforms, could dictate the rapidity of inositol pyrophosphate turnover on a cell-to-cell basis. This in turn could influence the sensitivity with which levels of inositol pyrophosphates respond to appropriate stimuli. This is analogous to how differential expression of cAMP-phosphodiesterases isoforms influence cell-to-cell differences in the sensitivity of agonist-mediated cAMP signaling [22].

All human DIPPs behaved similarly to Ddp1p in exhibiting higher k_{cat} values for 1-InsP_7 compared to 5-InsP_7 and InsP_8 (Table 1). The K_m data only vary over a 4-fold range (35 to 148 nM), across every enzyme and every substrate. The demonstration that rates of InsP_7 dephosphorylation equal or exceed those of InsP_8 metabolism (Table 1) explains why so little InsP_7 accumulated when InsP_8 was incubated with DIPPs (Fig. 3); the InsP_7 was rapidly converted to InsP_6.

Our new kinetic data yield further conclusions: since cellular levels of 5-InsP_7 are about 1-2 μM [15,23], these can now be considered sufficient (see Table 1) to be at a saturating concentration for all DIPPs. The k_{cat} values for 5-InsP_7 dephosphorylation are 5 to 9-fold lower than those for 1-InsP_7 (Table 1). However, the affinities of the two InsP_7 isomers for DIPPs are similar (Table 1), so they will compete for the DIPP active sites in direct proportion to their cellular concentration ratios. In mammalian cells, steady-state levels of 1-InsP_7 are10 to15-fold lower than those of 5-InsP_7 [24]. Thus, *in vivo* it is unlikely that the steady-state rate of 1-InsP_7 dephosphorylation will be significantly greater than that for 5-InsP_7. The latter conclusion - which can only be made now that kinetic parameters are available (Table 1) - counters a recent proposal [21] that, *in vivo*, a preferential DIPP activity towards 1-InsP_7 “masks” its rate of kinase-mediated synthesis relative to that for 5-InsP_7.

3.3 Inositol pyrophosphates do not regulate the human homologue of the yeast Pho80/81/85 cyclin kinase complex

The debate over the relative functional significance of pathway I and II (see above) has been influenced by the observation [5] that, in yeast, 1-InsP_7 reversibly empowers Pho81 to

inhibit the Pho80/85 cyclin kinase complex. This remains the only demonstration to date that 1-$InsP_7$ serves a unique biological function. The mammalian homologs of Pho85 (the kinase), Pho80 (the kinase activator) and Pho81 (the kinase inhibitor) are, respectively, CDK5, p35 and CDK5RAP1 (originally: C42) [25,26]. However, unlike Pho81, there is no evidence recombinant CDK5RAP1 requires ancillary factors for inhibiting cyclin kinase activity [27].

In earlier experiments [6], 1-$InsP_7$ augmented inhibition of Pho85 by Pho81 when the latter was added at a molar ratio with Pho85 that was 20-30 fold lower that which, by itself, inhibited Pho85. In our CDK5 assays, we increased assay sensitivity by having CDK5RAP1 at the threshold level at which its own inhibitory effects can be detected (Fig. 4). We then added 4 μM 1-$InsP_7$, a concentration that is >20-fold higher than is physiological (see above); CDK5 activity was unaffected (Fig. 4B); $InsP_6$, 5-$InsP_7$ and $InsP_8$ were similarly ineffective (i.e. $p>0.05$ vs controls) (Fig. 4B). These data provide the first evidence that specific regulation of yeast cyclin kinase activity by 1-$InsP_7$ [5] is not conserved in mammals.

3.4 The positional specificity of DIPPs towards $InsP_8$

The positional specificity of DIPPs towards the 1- and/or 5-diphosphate groups on $InsP_8$ also influences relative fluxes through the inositol pyrophosphate pathways (Fig. 1). Positional specificity is difficult to quantify, as so little $InsP_7$ accumulates when $InsP_8$ is dephosphorylated by DIPPs (e.g. Fig 3). Furthermore,1-$InsP_7$ and 5-$InsP_7$ are not generally resolved by strong anion-exchange HPLC. However, the columns used in the current study yielded a partial separation, particularly when we collected smaller fractions from a shallower gradient (Fig. 5A).

During $InsP_8$ dephosphorylation by Ddp1p, DIPP1, DIPP2α and DIPP3α, the accumulation of new $InsP_7$ product was 45-70% above the level of the (predominantly) 1-$InsP_7$ that was present in the no-enzyme assays (Fig. 5). Both the increase in $InsP_7$ peak height, and the larger degree of peak spreading, were sufficient to indicate accumulation of both 1-$InsP_7$ and 5-$InsP_7$. However, the k_{cat} data in Table 1 allow us to conclude that, in these experiments (Fig. 5), 1-$InsP_7$ that is formed from $InsP_8$ will be degraded faster than the 5-$InsP_7$ that is produced. That is, the rate of the 5-phosphate removal from $InsP_8$ (yielding 1-$InsP_7$) is underestimated relative to the rate of 1-phosphate removal from $InsP_8$ (producing 5-$InsP_7$). This conclusion is confirmed by data in Fig. 6, which show DIPP1 metabolizes 1-$InsP_7$ faster than 5-$InsP_7$ from a 1:1 mixture. Thus, where the data allow us to determine positional specificity (Fig. 5), we conclude Ddp1p/DIPPs preferentially (but not exclusively) remove the 5-phosphate from $InsP_8$. Positional specificity for DIPPs 2β/3β was less clear (Figs 3), but based on sequence conservation and kinetic similarities, it seems likely they also show positional selectivity for the 5-phosphate on InsP_8. Thus, the preferential route of $InsP_8$ dephosphorylation is metabolically distinct from the main pathway for $InsP_8$ synthesis. This contrasts with the old idea [28] that DIPPs remove from $InsP_8$ the diphosphate group that is added after 5-$InsP_7$ (now known to be in the 1-position [29]). The latter conclusion arose from a different experimental approach in which commercially-prepared substrates were incubated with liver homogenates. It is unclear why the earlier experiments led to a different conclusion - current concern over the quality of the substrates used (see Section 1) could be relevant here - but the possibility of a separate $InsP_8$ phosphatase is another option that bears some consideration.

3.5 Concluding Comments

Our study increases insight into inositol pyrophosphate turnover and function *in vivo* by providing the first kinetic characterization of Ddp1p/DIPP-mediated hydrolysis of 1-$InsP_7$,

5-$InsP_7$ and $InsP_8$. Our results lead us to argue against previous suggestions [11,21] (made in the absence of the relevant kinetic data) that DIPPs conceal the importance of pathway II (see Fig. 1) by masking the rate of PPIP5K-driven phosphorylation of $InsP_6$ to1-$InsP_7$. Furthermore, much of the attention given to the functional significance of pathway II arises from evidence that 1-$InsP_7$ inhibits the yeast Pho85 cyclin kinase [5,6]. Our data (Fig. 4) indicate that this mechanism is not conserved in mammals. Indeed, in mammals the 5-$InsP_7$ that is produced by pathway I has functional significance, by competing with PtdIns(3,4,5)P_3 for PH domains [8,9]; 1-$InsP_7$ is much less potent [8].

The DIPP/Ddp1 family can also hydrolyze inorganic polyphosphates [21], 5-phosphoribosyl 1-pyrophosphate [30] and nucleotide dimers [16]. However, these particular catalytic activities are unlikely to affect the conclusions reached in this study, as they have alkaline pH optima and are orders of magnitude slower than the rates of inositol pyrophosphate hydrolysis.

Although mammalian cells contain only submicromolar levels of 1-$InsP_7$ (Section 3.2), its concentration in *S. cerevisiae* has been argued to reach 30 μM in phosphate-starved cells [5]. While others have disputed that claim [21], it has nevertheless been reported that, in ddp1Δ yeast, levels of (presumably) 1-$InsP_7$ were elevated 5-fold upon inhibition of Kcs1p by TNP, or by kcs1 deletion [11]. Those experiments were proposed to reveal the true extent of steady-state 1-$InsP_7$ synthesis, again arguing that Pathway II is underappreciated. However, perhaps in those experiments, Vip1p's phosphorylation of $InsP_6$ was artificially enhanced merely because of the absence of the kinase's preferred (and competing) substrate, 5-$InsP_7$ (see [20,29]).

Acknowledgments

RS Kilari was supported by a PhD studentship from the University of Wolverhampton's Research Institute of Healthcare Science. This research was also supported by the Intramural Research Program of the NIH, National Institute of Environmental Health Sciences.

References

1. Szijgyarto Z, Garedew A, Azevedo C, Saiardi A. Influence of inositol pyrophosphates on cellular energy dynamics. Science. 2011; 334:802–805. [PubMed: 22076377]
2. Shears SB. Diphosphoinositol polyphosphates: metabolic messengers? Mol Pharmacol. 2009; 76:236–252. [PubMed: 19439500]
3. Bhandari R, Saiardi A, Ahmadibeni Y, Snowman AM, Resnick AC, Kristiansen TZ, Molina H, Pandey A, Werner JK Jr, Juluri KR, Xu Y, Prestwich GD, Parang K, Snyder SH. Protein pyrophosphorylation by inositol pyrophosphates is a posttranslational event. Proc Natl Acad Sci U S A. 2007; 104:15305–15310. [PubMed: 17873058]
4. Shears SB, Gokhale NA, Wang H, Zaremba A. Diphosphoinositol polyphosphates: what are the mechanisms? Adv Enzyme Regul. 2011; 51:13–25. [PubMed: 21035493]
5. Lee YS, Mulugu S, York JD, O'Shea EK. Regulation of a cyclin-CDK-CDK inhibitor complex by inositol pyrophosphates. Science. 2007; 316:109–112. [PubMed: 17412959]
6. Lee YS, Huang K, Quiocho FA, O'Shea EK. Molecular basis of cyclin-CDK-CKI regulation by reversible binding of an inositol pyrophosphate. Nat Chem Biol. 2008; 4:25–32. [PubMed: 18059263]
7. Worley J, Luo X, Capaldi AP. Inositol Pyrophosphates Regulate Cell Growth and the Environmental Stress Response by Activating the HDAC Rpd3L. Cell Rep. 2013; 3:1476–1482. [PubMed: 23643537]
8. Gokhale NA, Zaremba A, Janoshazi AK, Weaver JD, Shears SB. PPIP5K1 Modulates Ligand Competition Between Diphosphoinositol Polyphosphates and PtdIns(3,4,5)P3 for Polyphosphoinositide-Binding Domains. Biochem J. 2013; 453:413–426. [PubMed: 23682967]

9. Chakraborty A, Koldobskiy MA, Bello NT, Maxwell M, Potter JJ, Juluri KR, Maag D, Kim S, Huang AS, Dailey MJ, Saleh M, Snowman AM, Moran TH, Mezey E, Snyder SH. Inositol pyrophosphates inhibit akt signaling, thereby regulating insulin sensitivity and weight gain. Cell. 2010; 143:897–910. [PubMed: 21145457]
10. Rohwer JM. Kinetic modelling of plant metabolic pathways. J Exp Bot. 2012; 63:2275–2292. [PubMed: 22419742]
11. Padmanabhan U, Dollins DE, Fridy PC, York JD, Downes CP. Characterization of a selective inhibitor of inositol hexakisphosphate kinases: Use in defining biological roles and metabolic relationships of inositol pyrophosphates. J Biol Chem. 2009; 284:10571–10582. [PubMed: 19208622]
12. Safrany ST, Caffrey JJ, Yang X, Bembenek ME, Moyer MB, Burkhart WA, Shears SB. A novel context for the "MutT" module, a guardian of cell integrity, in a diphosphoinositol polyphosphate phosphohydrolase. EMBO J. 1998; 17:6599–6607. [PubMed: 9822604]
13. Caffrey JJ, Safrany ST, Yang X, Shears SB. Discovery of Molecular and Catalytic Diversity Among Human Diphosphoinositol Polyphosphate Phosphohydrolases: An Expanding NUDT Family. J Biol Chem. 2000; 275:12730–12736. [PubMed: 10777568]
14. Hidaka K, Caffrey JJ, Hua L, Zhang T, Falck JR, Nickel GC, Carrel L, Barnes LD, Shears SB. An Adjacent Pair of Human NUDT Genes on Chromosome X are Preferentially Expressed in Testis and Encode Two New Isoforms of Diphosphoinositol Polyphosphate Phosphohydrolase. J Biol Chem. 2002; 277:32730–32738. [PubMed: 12105228]
15. Leslie NR, McLennan AG, Safrany ST. Cloning and characterization of hAps1 and hAps2, human diadenosine polyphosphate-metabolizing Nudix hydrolases. BMC Biochemistry. 2002; 3:20. [PubMed: 12121577]
16. Safrany ST, Ingram SW, Cartwright JL, Falck JR, McLennan AG, Barnes LD, Shears SB. The diadenosine hexaphosphate hydrolases from *Schizosaccharomyces pombe* and *Saccharomyces cerevisiae* are homologues of the human diphosphoinositol polyphosphate phosphohydrolase: Overlapping substrate specificities in a MutT motif. J Biol Chem. 1999; 274:21735–21740. [PubMed: 10419486]
17. Loss O, Azevedo C, Szijgyarto Z, Bosch D, Saiardi A. Preparation of quality inositol pyrophosphates. J Vis Exp. 2011:e3027. [PubMed: 21912370]
18. Capolicchio S, Thakor DT, Linden A, Jessen HJ. Synthesis of Unsymmetric Diphospho-Inositol Polyphosphates. Angew Chem Int Ed Engl. 2013; 52:6912–5916. [PubMed: 23712702]
19. Wu M, Dul BE, Trevisan AJ, Fiedler D. Synthesis and characterization of non-hydrolysable diphosphoinositol polyphosphate second messengers. Chem Sci. 2013; 4:405–410. [PubMed: 23378892]
20. Weaver JD, Wang H, Shears SB. The kinetic properties of a human PPIP5K reveal that its kinase activities are protected against the consequences of a deteriorating cellular bioenergetic environment. Biosci Rep. 2013; 33:228–241.
21. Lonetti A, Szijgyarto Z, Bosch D, Loss O, Azevedo C, Saiardi A. Identification of an evolutionarily conserved family of inorganic polyphosphate endopolyphosphatases. J Biol Chem. 2011; 286:31966–31974. [PubMed: 21775424]
22. Houslay MD. Adaptation in cyclic AMP signalling processes: a central role for cyclic AMP phosphodiesterases. Semin Cell Dev Biol. 1998; 9:161–167. [PubMed: 9599411]
23. Ingram SW, Safrany ST, Barnes LD. Disruption and overexpression of the *Schizosaccharomyces pombe aps1* gene and the effects on growth rate, morphology, and intracellular diadenosine 5′, 5‴-P^1, P^5-pentaphosphate and diphosphoinositol polyphosphate concentrations. Biochem J. 2003; 369:519–528. [PubMed: 12387729]
24. Lin H, Fridy PC, Ribeiro AA, Choi JH, Barma DK, Vogel G, Falck JR, Shears SB, York JD, Mayr GW. Structural analysis and detection of biological inositol pyrophosphates reveals that the VIP/PPIP5K family are 1/3-kinases. J Biol Chem. 2009; 284:1863–1872. [PubMed: 18981179]
25. Ching YP, Pang AS, Lam WH, Qi RZ, Wang JH. Identification of a neuronal Cdk5 activator-binding protein as Cdk5 inhibitor. J Biol Chem. 2002; 277:15237–15240. [PubMed: 11882646]

26. Huang D, Patrick G, Moffat J, Tsai LH, Andrews B. Mammalian Cdk5 is a functional homologue of the budding yeast Pho85 cyclin-dependent protein kinase. Proc Natl Acad Sci U S A. 1999; 96:14445–14450. [PubMed: 10588725]

27. Ching YP, Qi Z, Wang JH. Cloning of three novel neuronal Cdk5 activator binding proteins. Gene. 2000; 242:285–294. [PubMed: 10721722]

28. Shears SB, Ali N, Craxton A, Bembenek ME. Synthesis and metabolism of *bis*-diphosphoinositol tetrakisphosphate *in vitro* and *in vivo*. J Biol Chem. 1995; 270:10489–10497. [PubMed: 7737983]

29. Wang H, Falck JR, Hall TM, Shears SB. Structural basis for an inositol pyrophosphate kinase surmounting phosphate crowding. Nat Chem Biol. 2012; 8:111–116. [PubMed: 22119861]

30. Fisher DI, Safrany ST, McLennan AG, Cartwright JL. Nudix hydrolases that degrade dinucleoside and diphosphoinositol polyphosphates also have 5-phosphoribosyl 1-pyrophosphate (PRPP) pyrophosphatase activity that generates the glycolytic activator ribose 1,5-bisphosphate. J Biol Chem. 2002; 277:47313–47317. [PubMed: 12370170]

Highlights

- Understanding inositol pyrophosphate turnover through kinetic study of Ddp1p/DIPPs
- k_{cat} values for 1-InsP_7 are 5-20 fold higher than those for 5-InsP_7 and InsP_8
- InsP_7 does not regulate CDK5, the human homologue of the yeast Pho85 cyclin kinase
- Kinetics imply differential expression of DIPP isoforms sets signaling sensitivity
- Metabolically and functionally separate routes for InsP_8 synthesis and hydrolysis

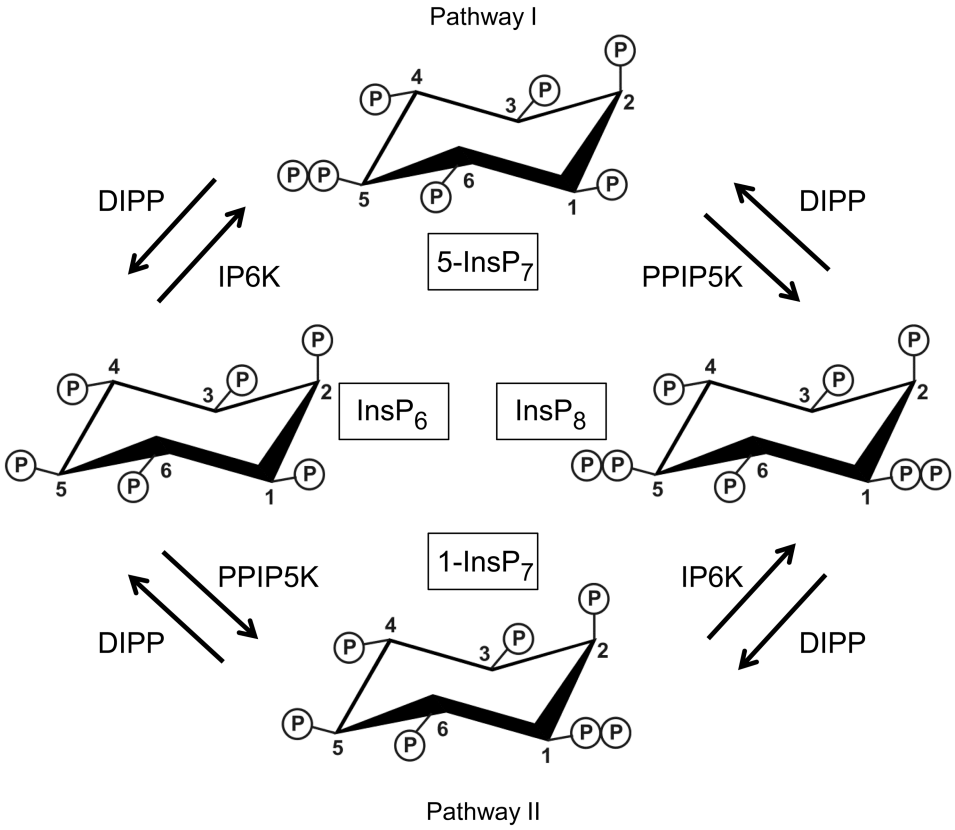

Figure 1. Metabolic interconversions of $InsP_6$, $InsP_7$and $InsP_8$

DIPP = Diphosphoinositol polyphosphate phosphohydrolase (Ddp1p in yeast); IP6K = inositol hexakisphosphate kinase (Kcs1p in yeast); PPIP5K = Diphosphoinositol polyphosphate kinase (Vip1p in yeast). Pathways I and II are named as in [11].

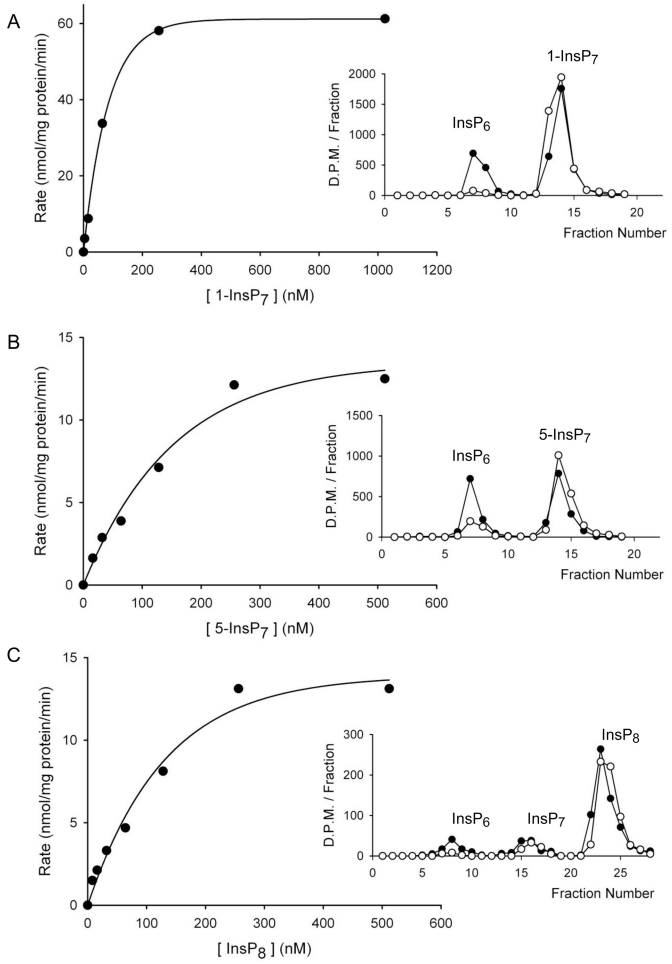

Figure 2. Analysis of the catalytic activities of Ddp1p

HPLC was used to obtain substrate saturation plots for Ddp1p against either A, 1-$InsP_7$, (0-1024 nM incubated with 2 ng Ddp1p for 0-25 min); B, 5-$InsP_7$ (0-512 nM incubated with 8 ng Ddp1p for 0-25 minutes); or C, $InsP_8$, (0-512 nM incubated with 8 ng Ddp1p for 0-25 min). Insets provide illustrative HPLC analyses using protocol 1 (Section 2.2): A, 10 nM 1-$InsP_7$, 20 ng Ddp1p, 10 min (not used in the substrate saturation plot). B 10 nM 5-$InsP_7$, 10 ng Ddp1p, 6 min (not used in the substrate saturation plot). C, 16nM $InsP_8$, 8ng Ddp1p, 4 min.

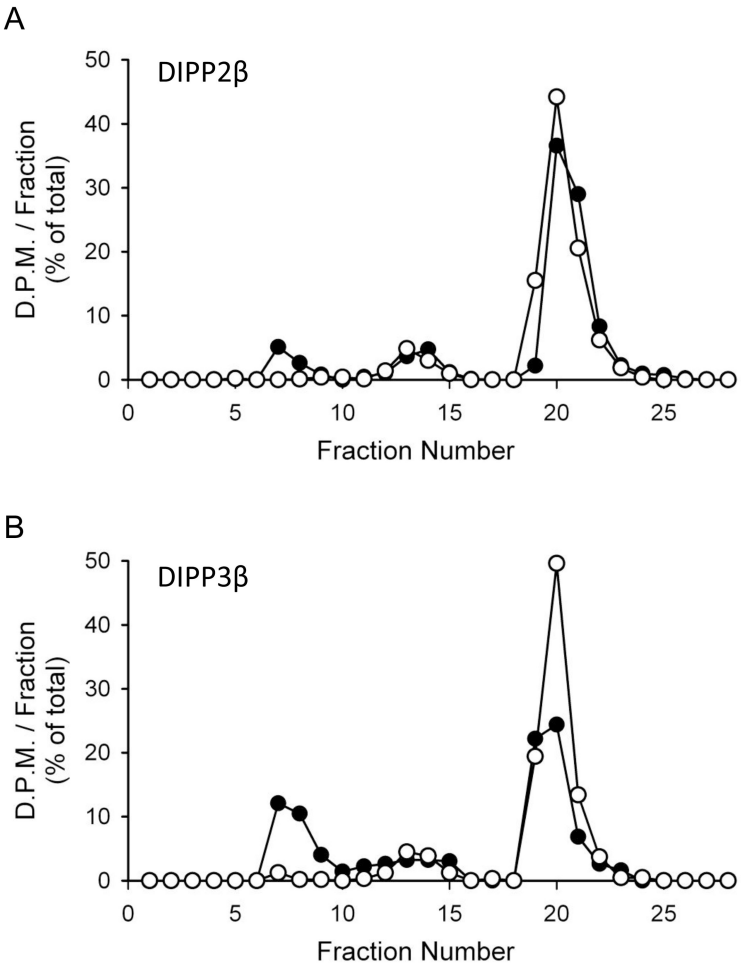

Figure 3. HPLC analyses of the hydrolysis of $InsP_8$ by DIPP2β and DIPP3β

HPLC analyses (protocol 1; Section 2.2) of the metabolism (filled circles) at 37°C of 16 nM $InsP_8$ incubated with (A) 10 ng DIPP2β for 6 min, or (B) 22.5 ng DIPP3β for 2 min. Open circles depict zero-time controls.

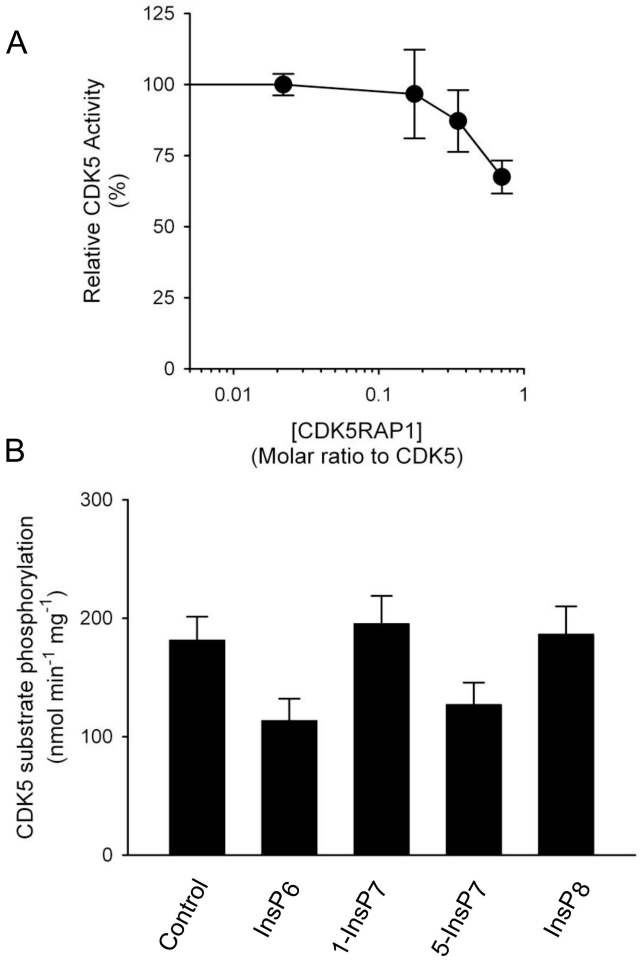

Figure 4. Inositol pyrophosphates do not regulate CDK5 activity

Panel A describes the concentration-dependent inhibition of CDK5 activity by CDK5RAP1, measured as described in Section 2. In panel B the molar ratio of CDK5RAP1:CDK5 was 0.4:1. None of the added inositol phosphates (4 μM) affected CDK5 activity ($p>0.05$ vs vehicle control; analysis by ANOVA with a Dunnett's post hoc test, n=5-8). Further experiments (not shown) did not uncover “order-of-addition” effects upon CDK5 activity.

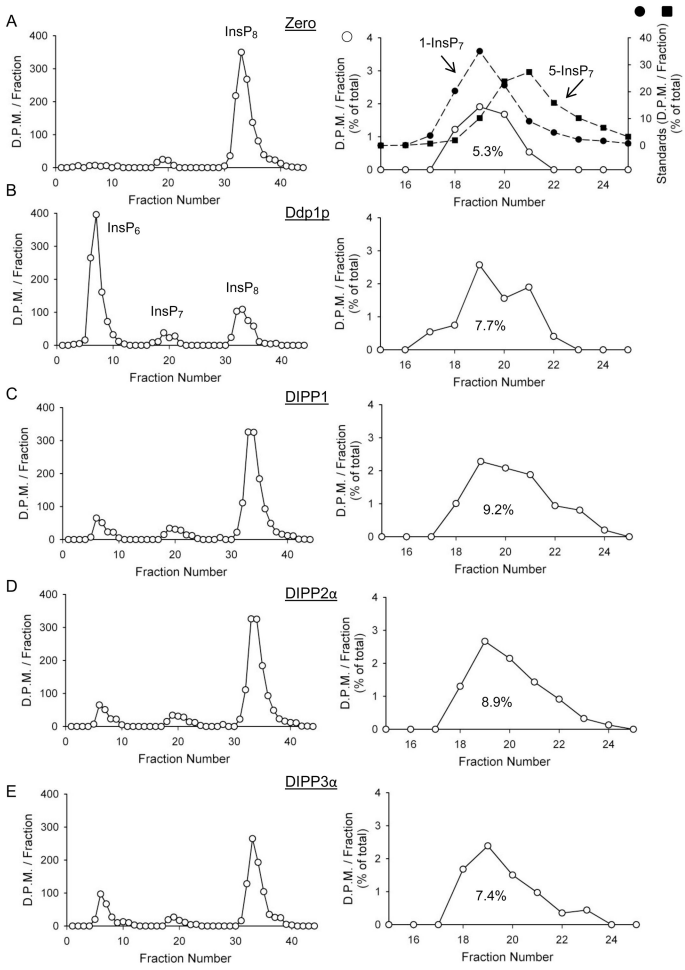

Figure 5. HPLC analyses of $InsP_8$ dephosphorylation by Ddp1p, DIPP1, DIPP2α and DIPP3α

Representative HPLC runs (protocol 2; Section 2.2) are shown for reactions containing either no enzyme (A; "zero"), or B, 16 ng Ddp1p, C, 2 ng DIPP1, D, 20ng DIPP2α and E, 10ng DIPP3α, all incubated for 8 min with 16 nM $InsP_8$. The right hand panels in each pair amplify the $InsP_7$ region of the chromatograph (open circles; $InsP_7$ is quantified as percentage of total); filled symbols show elution of 1-$InsP_7$ and 5-$InsP_7$ standards (determined individually).

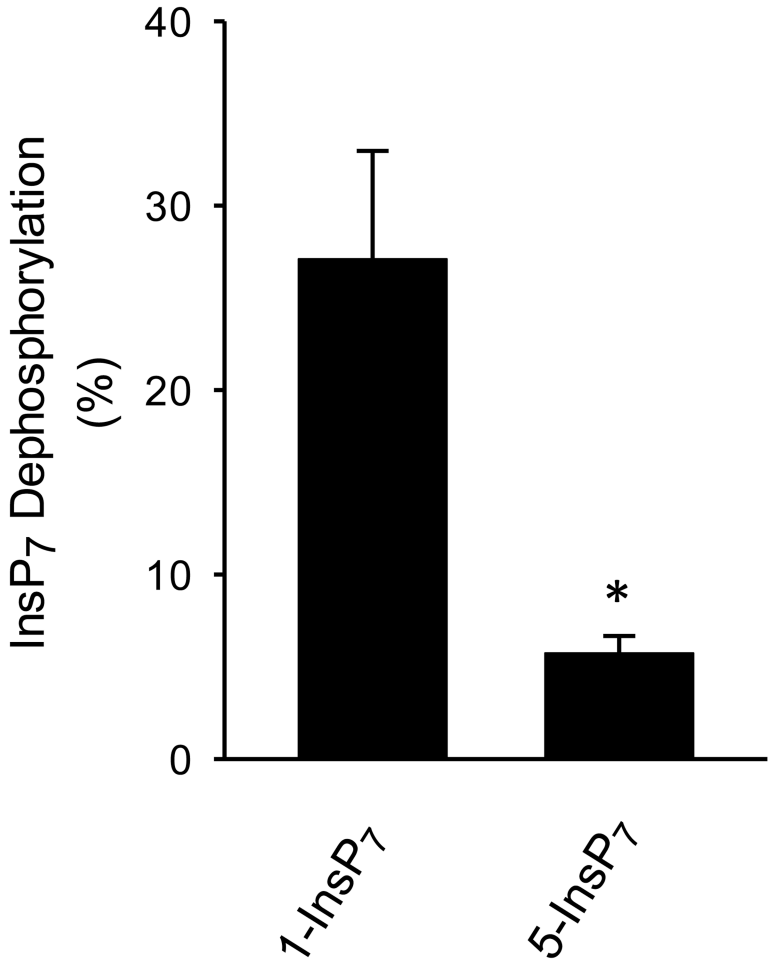

Figure 6. Metabolism of a 1:1 mixture of 1-InsP$_7$ and 5-InsP$_7$ by DIPP1

1-InsP$_7$ plus 5-InsP$_7$ (10 nM each) were together incubated for 10 min with 0.3 ng DIPP1 plus approx 1000 D.P.M. of either 1-[^{3}H]InsP$_7$ (left hand bar) or 5-[^{3}H]InsP$_7$ (right-hand bar). HPLC analysis determined the metabolism of each InsP$_7$. *p=0.02 (t-test; n=3).

Table 1

Ddp1p/DIPP kinetic data

	1-InsP$_7$		5-InsP$_7$		InsP$_8$	
	K_m (nM)	$10^2 \times k_{cat}$ (s^{-1})	K_m (nM)	$10^2 \times k_{cat}$ (s^{-1})	K_m (nM)	$10^2 \times k_{cat}$ (s^{-1})
Ddp1p	105	2.4 ± 0.05	93	0.4 ± 0.1	148	0.5 ± 0.1
DIPP1	42	110 ± 30	52	13 ± 3	85	10 ± 2
DIPP2α	60	5 ± 2	35	0.7 ± 0.2	55	0.24 ± 0.08
DIPP2β	70	1.7 ± 0.5	40	0.3 ± 0.09	42	0.16 ± 0.02
DIPP3α	104	23 ± 2	146	4 ± 2	126	2.2 ± 0.4
DIPP3β	73	8 ± 2	63	0.88 ± 0.07	78	0.37 ± 0.06

Kinetic data were obtained as described in Section 2. Average (n=3-5) substrate affinities were first compiled as -log K_m (SEMs were <3% of the mean) and then transformed to K_m for the Table.

FEBS Lett. Author manuscript; available in PMC 2014 November 01.